



Section 9. Materials processing, fabrication, inspection and maintenance

Magnetic non-destructive evaluation of accumulated fatigue damage in ferromagnetic steels for nuclear plant component

K. Morishita ^{*}, A. Gilanyi, T. Sukegawa, T. Uesaka, K. Miya

Nuclear Engineering Research Laboratory, The University of Tokyo Tokai, Naka-gun, Ibaraki 319-11, Japan

Abstract

We performed the measurement of magnetic properties of ferromagnetic steels that were degraded by tensile plastic deformation and cyclic loading, where lattice imperfections were produced in the steels. Magnetic hysteresis curves were changed depending on the load conditions. The changes in coercive force, residual magnetic flux density and permeability were obtained as functions of the magnitude of residual strain for the tensile tests and the number of loading cycles for the fatigue test. In the case of the tensile deformation, the coercive force increased and the residual magnetic flux density decreased with increasing the residual strains. In the case of fatigue damage accumulated by the cyclic loading, the residual magnetic flux density decreased with increasing the number of cyclic loading, while the coercive force remained constant. The changes in hysteresis curves were well consistent with the transmission electron microscopy (TEM) observation results of microstructural changes in the steels. We concluded that the magnetic property was enough sensitive to microstructural changes caused by mechanical deformation. © 1998 Elsevier Science B.V. All rights reserved.

1. Introduction

First wall materials of a nuclear fusion reactor are subject to damage due to heavy neutron irradiation, thermal stress and plasma particle injection during an operation of the reactor. In order to establish a reliable fusion reactor plant, development of the following fusion material technologies is considered to be required: (1) a technology to predict material behavior under irradiation environment for materials design and selection, (2) a technology to inspect the integrity of structural components in the reactor plant [1], and (3) a technology for material recovery system to extend reactor lifetime for economical reason. In the present study, we focused on the second requirement for establishment of nondestructive evaluation method to precisely monitor changes in mechanical properties of the

materials from the viewpoint of ensuring the reliability of the plant.

Magnetic non-destructive evaluation (NDE) approach [1] is one of the most interesting topics in the field of nondestructive inspection and examination, since magnetic properties are greatly sensitive to microstructural changes in ferromagnetic materials through the microscopic interaction between magnetic moments and lattice defects. The magnetic inspection technologies suggested recently, are represented by a magnetic hysteresis measurement, a Barkhausen noise (BHN) analysis [2] and a SQUID sensor [3]. All the approaches could be promising for detailed description of degraded materials. However, physical models that show a correlation between the magnetic and mechanical properties, have not yet been established. The changes in the magnetic and mechanical properties is considered to be described as a function of microstructural changes in materials due to irradiation. A final goal of the present study is to establish a correlation among them in order to develop a nondestructive technique using the magnetic approach. In the present study, in order to investigate a possibility of application of the approach to integrity evaluation of ferromagnetic steels, we mea-

^{*} Corresponding author. Present address: Research Institute for Applied Mechanics, Kyushu University, Kasuga, Fukuoka 816, Japan. Tel.: +81 92 583 7718; fax: +81 92 583 7690; e-mail: mori@riam.kyushu-u.ac.jp.

sured magnetic property changes in damaged ferromagnetic A533B steels, the typical material of light water reactor pressure vessel.

2. Experimental

We measured magnetic properties of ferromagnetic steels that were degraded by plastic deformation or accumulated fatigue damage. The specimen was prepared for the present investigation from the A533B low alloy steel supplied by the Japan Steel Works. The plate-shape and cylindrical-shape specimens were manufactured from the steel in the case of the tensile and fatigue tests, respectively. Dimensions of the effective region of the plate-shape specimen were 70 mm in length, 30 mm in width and 5 mm in thickness. Effective diameter of the cylindrical-shape specimen was 8 mm.

Tensile tests were performed with constant strain rate of 0.3 $\mu\text{m}/\text{sec}$ at room temperature in a 200 kN servo-hydraulic testing system at the tensile range from the elastic to plastic deformation. The maximum tensile stresses at the test were 462, 550, >550, 580, 663 MPa, that corresponded to 0%, 0.378%, 0.43%, 2.9% and 7.45% of residual strains, respectively. Here, the specimens are denoted by specimen-B, -C, -D, -E and -F, respectively. The specimen-A denotes an initial condition before the tensile test.

The cylindrical-shape specimens were damaged by zero-tension cyclic load with a 50 kN servo hydraulic system. Load control was applied for the fatigue test with a sinusoidal wave form at a series of constant load amplitudes of 538, 542 and 546 MPa as maximum stresses that did not exceed the yield stress of the steel ($\sigma_y = 560$ MPa). The condition of the tests are listed in Table 1.

Our TEM (transmission electron microscopy) observation study showed the two phases in the A533B steels that were quenched by water from annealing temperature of 1133–1163 K for 145 min, followed by tempering process at 923–938 K for 139 min: One of the phases was a ferrite phase (α_1) with very high density of

dislocations which was originally a martensite phase before the tempering process. Another phase was a ferrite phase (α_2) with very few dislocations included. The α_2 phase could originate from a residual austenite phase before the tempering process. The amount of the α_1 phase was as much as that of the α_2 phase in the steel.

After the tension or fatigue tests, the specimens were unloaded, and thereafter, magnetized by a pair of yokes made of purified iron (99.99%), which were attached on the damaged specimens. The magnetic property of the damaged specimen was measured repeatedly at the same time to avoid the effect of specimen positioning against the yokes. A magnetic measurement system used for the present investigation is schematically shown in Fig. 1. The excitation current in copper wires of a coil wound around the yokes would produce a magnetic field, H , in the specimens, which would induce the specimens magnetized. The magnitude of the time derivation of a magnetic flux density, dB/dt , were picked up by another coil wound around the specimens. A plot of the magnetic flux density, B , versus the applied magnetic field, H , showed a magnetic hysteresis loop (so-called a $B-H$ curve), and its shape might reflect microstructures in the material. The frequency of the applied magnetic field was relatively low (0.5–0.05 Hz) in order to minimize eddy current effects [2] on the $B-H$ curve.

3. Magnetic property changes due to plastic deformation

Fig. 2 shows $B-H$ curves obtained from the plate-shape specimens that were damaged by the tensile tests. An inset in the figure represents a load–deformation diagram ($\sigma-\epsilon$ curve) of the specimen. The shape of the curve shows a typical diagram for soft-ferritic steel. The load condition of the experiment is also represented in the inset; The specimen-B was deformed up to elastic region. The specimen-C and -D were deformed up to yield strain occurred, where the Luders band were in propagation in the specimens. The specimen-E and -F were deformed up to work hardening occurred. An

Table 1
Experimental load condition in the present study

| ID | Tensile test | | Fatigue test |
|----|------------------------------|---------------------|------------------------------|
| | Maximum tensile stress (MPa) | Residual strain (%) | Maximum tensile stress (MPa) |
| A | 0 | 0 | 538 |
| B | 462 | 0 | 542 |
| C | 550 | 0.378 | 546 |
| D | >550 | 0.43 | |
| E | 580 | 2.9 | |
| F | 663 | 7.45 | |

Yield stress of the A533B steel is 560 MPa.

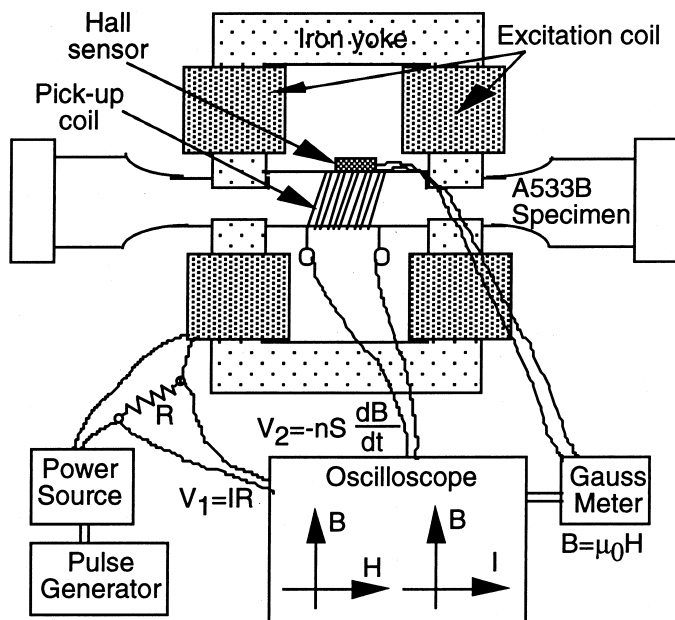


Fig. 1. Schematic representation of magnetic measurement system. Specimens are magnetized by a pair of yokes made of purified iron. Time derivative of magnetization is picked up with copper wire coils wound around specimens.

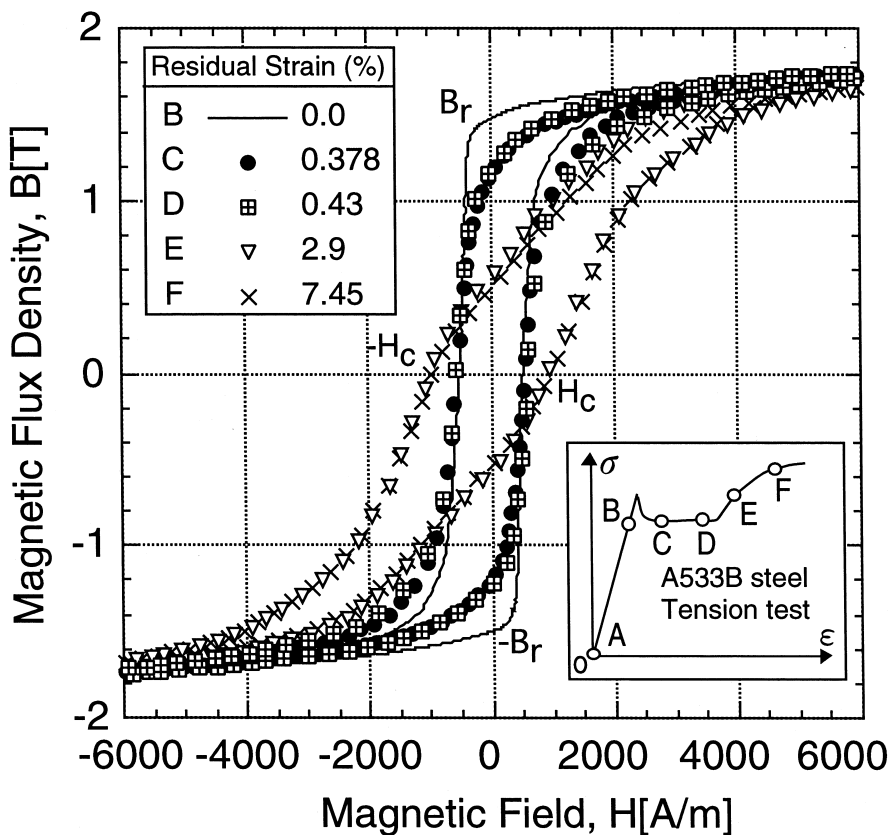


Fig. 2. Magnetic hysteresis loops for tensile deformation. Shape of the loops is changed depending on the deformation.

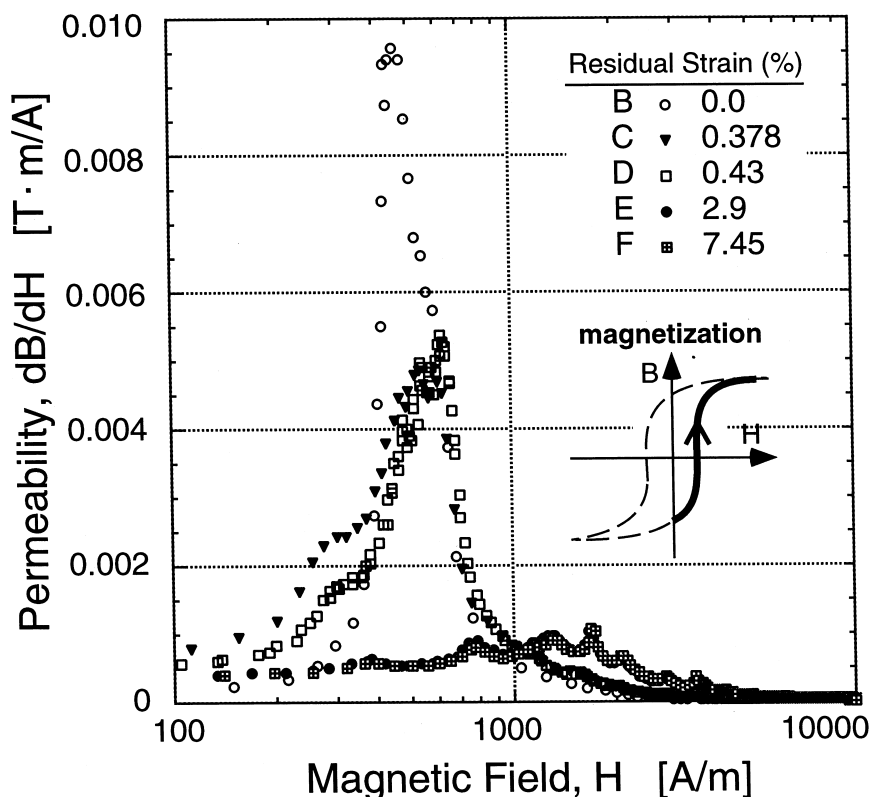


Fig. 3. Permeability during magnetization process of tensile test specimen as a function of residual strain. Peak of permeability decreases with increasing residual strain.

elastic tensile deformation had no effect on the shape of the B - H curve. However, the plastic deformation changed the shape of the curves, depending on the magnitude of the residual strain; Compared with the initial value before the tensile test, residual magnetic flux density, B_r , decreased for the specimens-C, -D, -E and -F. Coercive force, H_c , increased for the specimens-E and -F. A time derivation of the magnetic flux density, dB/dH , versus the applied field, H , is plotted in Fig. 3 for the magnetization process as a function of the residual strain. The figure shows that the peak of the curve decreased with increasing the residual strain for the lower part of the applied field, H ($0 < H < 1000$ A/m), indicating that magnetizing process was more difficult to proceed during these applied field range in the case of higher residual strain, probably because of the existence of some defects that were introduced by mechanical tensile deformation [4]. In the case of work hardening (specimen-E and -F), the peak finally disappeared in the lower part of the applied field. However, during the higher part of the applied field ($H > 1000$ A/m), the magnetization proceeded due to greater applied field, while the magnetizing process seemed to be almost saturated in the case of lower residual strain.

Fig. 4 shows changes of permeabilities, dB/dH , during a demagnetization process as a function of the residual strain in the case of the tensile tests. As the applied field decreased, the permeability increased at greater applied field in the case of higher residual strain.

4. Magnetic property changes due to accumulated fatigue damage

Magnetic hysteresis loops were obtained from the cylindrical-shape specimens that were damaged by sinusoidal cyclic loading between zero and constant maximum tensile stress below the yield stress [5]. The residual magnetic flux density, B_r , decreased with the number of the fatigue cycles as shown in Fig. 5, while the coercive force was not changed during all through the cycles in the present investigation. The dependence of the magnetic flux density, B_r , was drastically different between 542 and 546 MPa. This might reflect the fact that the applied stress in the experiment was very near the average value of yield stress of the material, 560 MPa. The permeabilities, dB/dH , for the fatigue specimens indicated that the accumulated damage made the

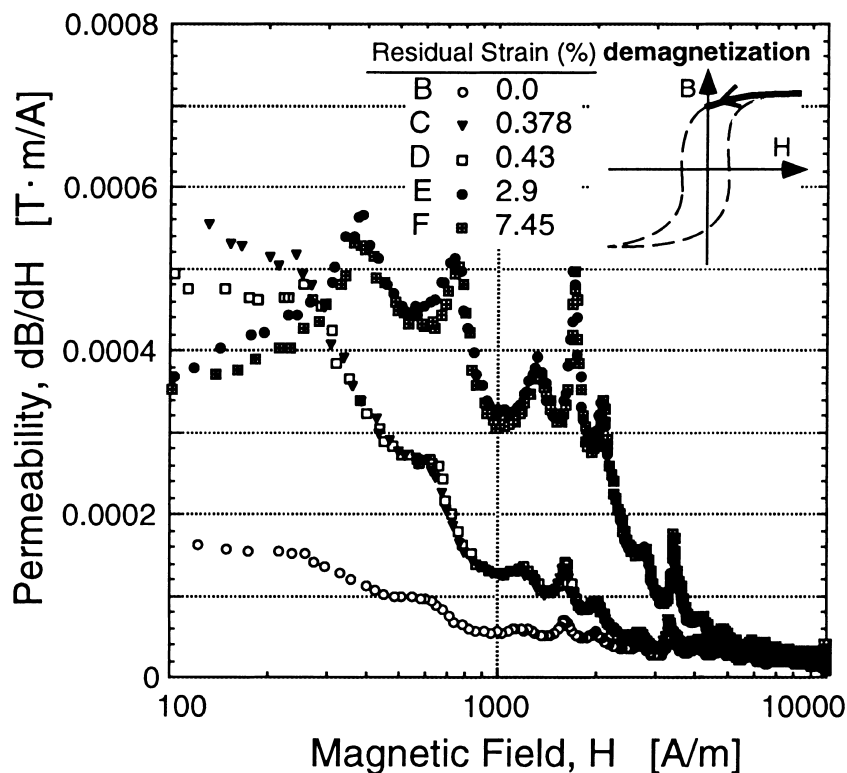


Fig. 4. Permeability during demagnetization process of tensile test specimen as a function of residual strain. Magnitude of permeability increases with decreasing applied field.

magnetization process more difficult for the greater number of fatigue cycles; The magnitude of the permeabilities decreased with increasing the number of fatigue cycles. However, in contrast with the work hardening cases (specimen-E and -F), the peaks at greater applied field disappeared in the permeabilities change.

A TEM observation showed an increase in the number density of dislocations at the α_2 phase of the material with increasing the fatigue cycles, which was qualitatively consistent with the magnetic property change [6].

5. Discussion

The permeabilities during the magnetization and demagnetization processes showed a clear effect of the damage due to plastic deformation and cyclic loading. In both cases, the results of the magnetic measurements indicated that, with increasing the mechanical damage, the magnitude of the permeabilities decreased at the lower part of the applied field ($0 < H < 1000$ A/m), where magnetic domain wall was considered to move [2]. Our TEM observation showed an increase in the num-

ber density of dislocations at the α_2 phase of the steel for both the tensile and fatigue tests. The dislocations could play an important role as obstacles to the magnetization, which was well consistent with the published work in the literature [7,8]. However, a decrease in the permeabilities had no effect on a change in the coercive force for both the tests, except the case of the work hardening of the tensile test.

The TEM observation also showed so-called the 'cell structure' of dislocations in the case of the work hardening, where the coercive force increased and the residual magnetic flux density decreased. As shown in Fig. 3, the permeability during the magnetization process was quite small for the work hardening case, indicating that the movement of the domain wall could be perfectly obstructed by the cell structure of dislocations. The domain wall movement is considerably a collective motion of magnetic moment of atoms, which could be prohibited from moving by the large assembly of dislocations as the cell structure. In this case, greater applied field could be required for the wall movement. In Fig. 3, peaks of the permeability curve was observed to move into the higher part of the field. The peak shift would bring an increase in the coercive force as shown in Fig. 2.

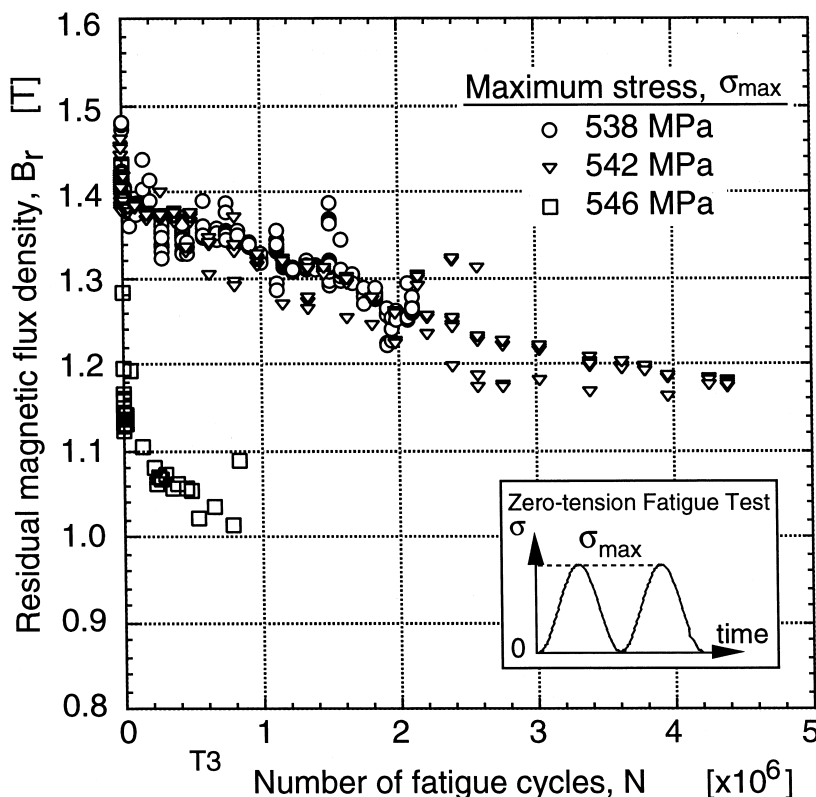


Fig. 5. Dependence of residual magnetic flux density on number of fatigue cycles as a function of applied maximum stress of fatigue tests.

As the applied field increases and overcomes the minimum force that is required for magnetic moments to turn into a different direction from the so-called easy axis, the magnetization proceeds by rotation of the magnetic moment. After the magnetization saturated, during the demagnetization process, the direction of the moment could start to rotate back into the easy axis. Fig. 4 shows that the demagnetization process proceeds at higher applied field in the case of larger residual strain where more dislocations might exist. The mechanically induced dislocations would produce strain fields around them and prohibit magnetic moment of each atom from turning into the easy axis, with a result of a decrease in the residual flux density, B_r . Therefore, during the demagnetization process, the number density of dislocations, rather than the global structure of dislocations as the cell structure, would be more important for the magnetic property changes. An increase in the density number of dislocations would change the residual flux densities that are mainly determined by the rotation of the moment.

We found in the present investigation that the magnetic approach can detect, at least, a difference between an increase in the number of dislocations and their cell

structure, showing a higher sensitivity of the magnetic property to the dislocations. Our Vickers hardness measurement did not detect the present fatigue damage at all. Whether the irradiation degradation [9–12] of the A533B steels can be detected by the magnetic approach is not so clear. However, it is very interesting to investigate the possibility of application of the present approach to the irradiation degradation problem.

6. Conclusion

Magnetic property measurements were performed for the A533B pressure vessel steels that were mechanically damaged by the tensile and fatigue tests. An increase in the number density of dislocations leads to a decrease in the residual magnetic flux density. A formation of cell structure of the dislocations, that was observed in the case of work hardening in the tensile test, obstructed the domain wall movement almost perfectly, leading to an increase in the coercive force. We concluded that the magnetic property is enough sensitive to microstructural changes caused by mechanical damage.

Acknowledgements

The work is performed within the activities developed by one of the committees of The Japan Society of Applied Electromagnetics and Mechanics (JSAEM), Tokyo, Japan. Part of the work is supported by the program for young scientists from the 'JUPITER' Monbusho-US DOE collaboration.

References

- [1] S.R. Doctor, D.M. Boyd, S.M. Bruemmer, Nucl. Eng. Des. 118 (1990) 355.
- [2] S. Chikazumi, Physics of Ferromagnetism, Shokabo Press, Tokyo, Japan, 1995.
- [3] R.C. Black, F.C. Wellstood, IEEE Trans. Appl. Superconductivity 5 (1995) 2137.
- [4] A. Seeger, H. Kronmuller, O. Boser, M. Rapp, Phys. Stat. Sol. 3 (1963) 1107.
- [5] A. Gilanyi, K. Morishita, T. Sukegawa, M. Uesaka, K. Miya, Proceedings of the Fourth International Symposium on Fusion Nuclear Technology (ISFNT-4), 1997, Tokyo, Japan, to be published in Fusion Eng. Design.
- [6] H. Mughrabi, R. Kutterer, K. Lubitz, H. Kronmuller, Phys. Stat. Solid. 38 (1975) 261.
- [7] H. Kronmuller, Canadian J. Phys. 45 (1967) 631.
- [8] A. Seeger, H. Kronmuller, H. Rieger, H. Trauble, J. Appl. Phys. 35 (1964) 746.
- [9] W.J. Phythian, C.A. English, J. Nucl. Mater. 205 (1993) 162.
- [10] J.T. Buswell, M.G. Hetherington, W.J. Phythian, G.D.W. Smith, G.M. Worrall, Proceedings of the International Symposium on Effects of Radiation on Materials, ASTM STP 1046, 1990, p. 127.
- [11] M.K. Miller, M.G. Burke, 16th International Symposium on Effects of Radiation on Materials, ASTM STP 1175, 1993, p. 492.
- [12] T.J. Williams, W.J. Phythian, Proceedings of the International Symposium on Effects of Radiation on Materials, ASTM STP 1270, 1996, p. 191.